DOI: 10.13009/EUCASS2022-7676
9TH EUROPEAN CONFERENCE FOR AERONAUTICS AND SPACE SCIENCES (EUCASS)

PERSEUS and Innovative Propulsion Laboratory Project The Mini Viserion rocket engine

Julien SENON, Julien SIMON** , Paul MARCHI***, Pascal PEMPIE**** et al.*
**Innovative Propulsion Laboratory, 94200, Ivry-sur-Seine, France*
julien.senon@ipsa.fr
***Innovative Propulsion Laboratory, 94200, Ivry-sur-Seine, France*
julien.simon@ipsa.fr
****Innovative Propulsion Laboratory, 94200, Ivry-sur-Seine, France*
paul1.marchi@ipsa.fr
*****PERSEUS, Coordinator, CNES, pascal.pempie@wanadoo.fr*

Abstract

Rocket engine ambient pressure adaptation has been a lasting difficulty in the aerospace domain. This paper aims to present a potential solution by enabling an engine to vary its expansion ratio in flight through the use of a continuously expanding nozzle. The development of a 5 kN regeneratively-cooled pressure-fed LOX/CH4 engine is explained. The design process of a pintle injection system, a regenerative cooling system, a thrust vector control apparatus as well as the adaptative nozzle is detailed. The goal of this engine is to be used both in the PERSEUS project and as a demonstrator for the innovative nozzle.

Nomenclature

Symbols

$\dot{W}$	Mass flow rate	h	Heat transfer coefficient
C_d	Pressure loss coefficient	TMR	Total Momentum Ratio
ρ	Density	λ	Thermal conductivity
P	Pressure	Re	Reynolds number
k_{inj}	Coefficient representing the pressure ratio upstream and downstream of the pintle	L	Length
D	Diameter	Z	Number of channels
Pr	Prandtl number	T	Temperature
m	Molecular mass	e	Wall thickness
γ	Heat capacity ratio	F	Thrust
C^*	Characteristic velocity	i	Mass flow rate
D_{hy}	Hydraulic diameter	V	Velocity
A	Surface area	S	Cross section surface
σ	Correction factor for property variations across the boundary layer	M	Mach number
μ	Dynamic viscosity	ε	Nozzle cross section ratio

Subscripts

th	Property at chamber throat
l	Coolant
$corr$	Corrected
g	Hot gases
c	Combustion chamber
wg	Gas-side wall condition
wl	Coolant-side wall condition
e	Nozzle outlet
amb	Ambient

DOI: 10.13009/EUCASS2022-7676

1. Introduction

One of the most well-known problems in the design of a rocket engine is the adaptation of the nozzle to the altitude range of use. Indeed, the efficiency of a rocket engine is maximum when the static pressure of the ejected gases is identical to the ambient pressure. This means that the engine is exploiting the energy potential of its propellants to the maximum. This engine outlet pressure is defined by the ratio of the cross-section between the tip of the nozzle and the nozzle throat. However, in most cases, this ratio cannot be modified due to the absence of a device adapted to the aerodynamic, thermal, and mechanical constraints generated by a rocket engine. This means that it is impossible to modify the engine output pressure for the same operating speed. Therefore, outside the altitude corresponding to the nozzle outlet pressure, the engine loses efficiency.

This is one of the reasons why all launchers are divided into several stages, allowing to start with an engine adapted to low altitudes and then to use a second one adapted to high altitudes or even vacuum. Indeed, rocket engine designers make a compromise by adjusting the output pressure to the average pressure that the craft will encounter during its use. This means that below and above the design altitude, efficiency is negatively impacted.

The solution proposed here the use of an adaptive divergent device, i.e. a nozzle capable of varying its cross-section and therefore its outlet pressure. Where an aerospike type nozzle becomes too complicated to cool and generates an increase in mass, the proposed device does not change the design method of a bell nozzle rocket engine. Another comparison can be made with the Vinci upper stage engine developed by Arianegroup, which has a nozzle extension. Although in their case the nozzle extension is to save space, one could imagine the engine operating in two modes, retracted, or extended. However, this would allow optimal operation only at two altitudes. Our adaptive nozzle is a truncated cone-shaped ring composed of a set of prismatic tiles extending the divergent nozzle. The translation of these tiles via an adapted deployment system allows the length of the divergent nozzle and therefore its outlet section to be varied continuously. This will allow the engine to have a defined range of operating altitudes as required.

2. Objective

This idea inspired the founding of the Innovative Propulsion Laboratory student association at the Institut Polytechnique des Sciences Avancées in 2019. This now-patented innovation is currently being implemented as part of the CNES PERSEUS student project on a MINERVA engine using a combination of LOX/CH4 propellants fed under pressure. Called Mini Viserion, this rocket engine with a nominal thrust of 5kN is entirely designed by IPL's teams. The medium-term objective is to prepare and carry out the first tests on a test bench at the end of 2022. The challenge is the experimental validation of the efficiency of this innovation and the production of a new rocket engine for the PERSEUS student project.

To succeed, the realization of this project has been conferred to several teams among the IPL, each of them dealing with different aspects of the design. The first part of the work concerns the engine's injection device, i.e. the development of a pintle-type injector allowing the propellants to be mixed efficiently in the combustion chamber. The second part concerns the development of the engine's cooling system, a purely regenerative circuit that does not use other techniques such as film cooling. The third part regards the characterisation and development of the adaptive nozzle and its deployment device. Finally, as the Mini Viserion is destined to equip the Astreos rockets of the PERSEUS project, the last part of the work concerns the design of a Thrust Vectoring Control (TVC) device, which allows the motor to be oriented and the rocket to be controlled using a gimbal.

3. Propellant injection system

In the context of this study, we will focus on the designing of an injection system capable of sustaining the Mini Viserion. The fundamental function of that system is to ensure maximal homogeneity between the two propellants in the desired mixture ratio. In this case the mixture ratio will be 2.7 [1]. Many different injector designs exist, each with their own advantages and drawbacks. In the case of the Mini Viserion, it has been decided quite early, and for several reasons that the most appropriate injector design would be a Pintle type injector. First, the mechanical complexity and designing difficulties are lower than other types of injectors. This injector type is also made for liquid-liquid injection, which will be the case in the Mini Viserion. Finally, by using this type of injector, there is potential for the integration of a throttling system in future revisions of this engine.

To design the injector, the first step was to compute the characteristic design specifications, the area of injection as well as the Total Momentum Ratio [2] [3], which are defined by the following relations:

DOI: 10.13009/EUCASS2022-7676

$$S = \frac{\dot{W}}{C_d\sqrt{2\rho P_c\left(k_{inj} - 1\right)}} \tag{1}$$

$$TMR = \frac{\dot{W}_{LOx}}{\dot{W}_{CH4}} \tag{2}$$

These results have allowed the design of a first iteration of the injection system, made up of the following components:

- The lid/cover (in brown)
- The injection plate containing 10 holes (in pink)
- The pintle itself, containing 64 holes distributed in two rows (in red).

The mass of the lid was then optimized in order to obtain the results shown below.

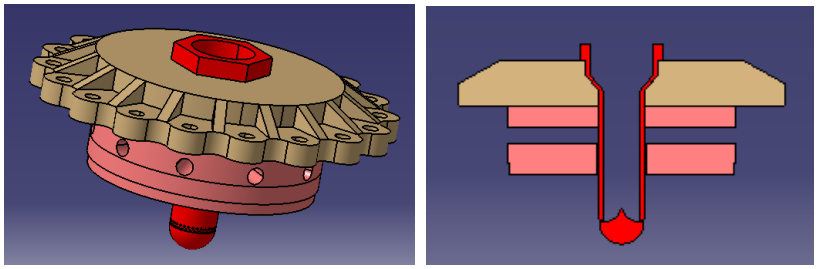

Figure 1: Isometric and sectional views of the pintle injection system

The next design stage was to verify and optimize the current geometry by running ANSYS simulations. The fluidic behaviour inside the injector plate and the pintle was studied and the value of the pressure drop coefficient, C_d, was obtained. The ejection velocities obtained using CFD confirmed the analytically calculated velocities.

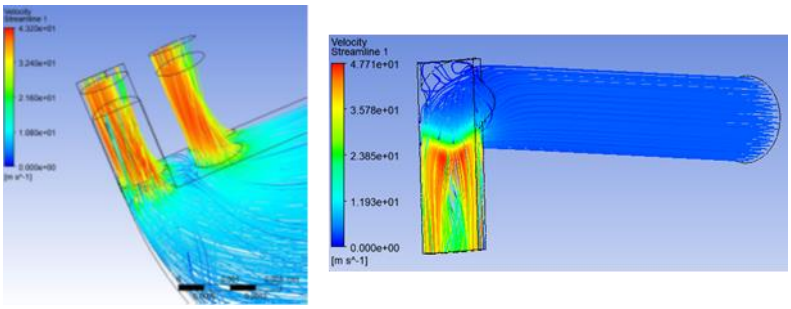

Figure 2: Observations of the current lines on the pintle and the injection plate

The next set of simulations' goal was to verify the structural integrity of the injection system. Also done using ANSYS, that step is of vital importance to check for any potential displacements or instabilities of the components inside the assembly. Copper was the material chosen for the injection plate and the pintle, given that it has a sufficient resistance to high temperatures as well as a high thermal conductivity and thermal diffusivity, which are essential for these components of the assembly. On the other hand, the lid will be made from nickel. The constraints on that part are much milder, which means that the part should simply be as light as possible while keeping an acceptable mechanical strength. The simulation results show that the entirety of the assembly is capable of withstanding the pressure conditions it will be subjected to.

DOI: 10.13009/EUCASS2022-7676

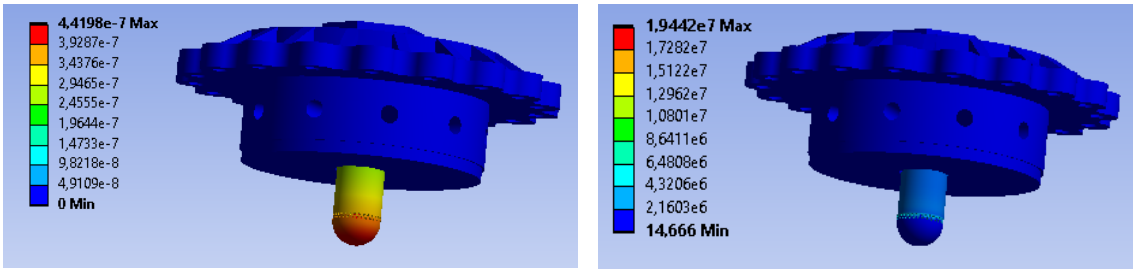

Figure 3: Result of simulations of total displacement and equivalent stress

As we anticipated, the part most exposed to the strong conditions is the tip of the central pintle. But the safety margin for the resistance of the parts is of about 30. This allows a lot of flexibility; however, it is essential to note that the thermal studies and simulations have not been done at this point in time since the current focus is on studies evaluating the quality of the atomization of the propellants. It will also be of major importance to analyse and simulate the combustion phenomena inside the combustion chamber to prevent issues during testing. Once all these studies will have been completed and their effects taken into account, it is likely that the safety margin will be lower.

4. Regenerative cooling

In a rocket engine, given that the temperatures in the combustion chamber are around and, in some cases, exceed 3500K, cooling considerations are of vital importance for the engine to work properly. Many different methods of cooling exist, one of the most widely used ones is regenerative cooling, which consists of making a coolant fluid flow in cooling channels around the chamber. For the Mini Viserion it has been established that regenerative cooling will not need to be combined with other cooling methods such as film cooling, since the cooling requirements of the engine are sufficiently low. It is possible to use the oxidizer (LOX) or the fuel (Methane) for cooling. To avoid oxidation inside the cooling channels, liquid methane will be used inside the regenerative cooling system.
For a successful design the cooling system, several major criteria are to be considered:

- Maximum allowable temperature of the chamber wall
- Pressure necessary at the injection
- Burnout heat-flux
- Fuel mass flow rate

The number, shape, and size of the cooling channels must be chosen such that the restrictions above are respected. It is important to note that the cooling channels will have a rectangular cross-section for ease of manufacturing.

4.1. Cool The Engine

To find a suitable channel configuration, different tests are done by varying their number, size and shape and calculating the resulting temperatures, heat flux and pressure loss using the python program *Cool the Engine* (CTE) that was created specifically for that purpose. The program includes a 2D heat transfer solver that calculates the temperature and heat flux at all points in the chamber wall between the channels and the hot gases as well as between the channels themselves. The pressure and temperature inside the chamber (that are used by the CTE) are computed by NASA's CEA, a Fortran program for computing chemical equilibrium in a combustion chamber.

By running this code many times and adjusting the parameters at each run, it was possible to obtain a configuration allowing all constraints to be respected together. The configuration that was selected has 60 cooling channels.

4.2. Calculation of heat flux

The heat transfer coefficient from the hot combustion gases to the chamber wall is computed using Bartz's equation:

$$h_g = \frac{0.026}{{D_{th}}^{0.2}} \frac{\mu^{0.2}}{Pr^{0.6}} \left(\frac{P_c}{C^*}\right)^{0.8} \left(\frac{D_{th}}{R_{th}}\right)^{0.1} \left(\frac{A_c}{A}\right)^{0.9} \sigma \tag{3}$$

The heat transfer coefficient from the chamber wall to the liquid methane is calculated using Colburn's formula:

DOI: 10.13009/EUCASS2022-7676

$$h_l = \frac{0.023\lambda_l Re^{0.8} Pr^{0.4}}{D_{hy}} \tag{4}$$

It is important to correct this coefficient by taking into account the fin effect using the following relation:

$$h_{l_{corr}} = h_l\left(\frac{Z \cdot L}{\pi}\right) + Z\left[2h_l\lambda\left(\frac{\pi D}{Z} - L\right)\right]^{\frac{1}{2}} \tag{5}$$

In case the heat flux is higher than a critical value called the burnout (or critical) heat flux, the cooling provided by the liquid methane drops significantly because of the formation of a vapor film between the hot wall and the liquid coolant. To avoid this phenomenon, it is necessary to compute the burn out heat flux in the cooling channels and check that the predicted heat flux never exceeds the critical value. The critical heat flux was computed using the data provided in [4] and [5].

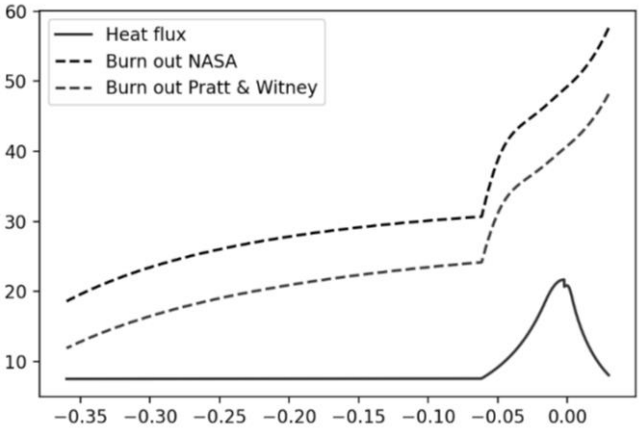

Figure 4: Heat fluxes along the engine length

4.3. Calculation of temperatures

The temperatures of the wall on the gas-side (T_{wg}) and coolant-side (T_{wl}) are determined using the formulas below:

$$T_{wg} = \frac{\frac{\lambda}{e}\left(h_g T_g + h_l T_l\right) + h_l h_g T_g}{h_l h_g + \frac{\lambda}{e}\left(h_l + h_g\right)} \tag{6}$$

$$T_{wl} = \frac{\frac{\lambda}{e}\left(h_g T_g + h_l T_l\right) + h_l h_g T_l}{h_g h_l + \frac{\lambda}{e}\left(h_g + h_l\right)} \tag{7}$$

Here are the temperatures computed by Cool the Engine, we can see that the wall temperatures are below the maximum allowable value (800K):

DOI: 10.13009/EUCASS2022-7676

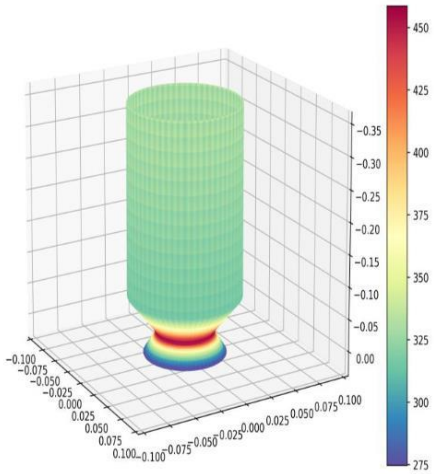

Figure 5: Heat distribution in gas-side chamber wall

More simulations will be required to guarantee that the heat flux from the hot radiatively-cooled nozzle extension does not cause too high temperatures in the copper at the point of contact.

4.4. Mechanical resistance of the cooling channels

Because of the high heat fluxes and large pressures inside the regenerative cooling system it is important to check that the structural integrity of the cooling channels isn't altered. This was done by running a thermomechanical simulation using the commercial simulation software ANSYS, using the results of the CTE as input for temperature and pressure. This simulation was done several times using different copper alloys for the walls between the cooling channels and the chamber in order the find the one that would have both a sufficient thermal conductivity and a mechanical strength capable of bearing the loads imposed by the conditions in the channels. This simulation was done on one channel only, to reduce computation time, since there is axial symmetry around the center line of the chamber. Results were found to be within expected values (constraints below 410 MPa) and confirmed that the copper alloy C15100 can be used for making the chamber walls.

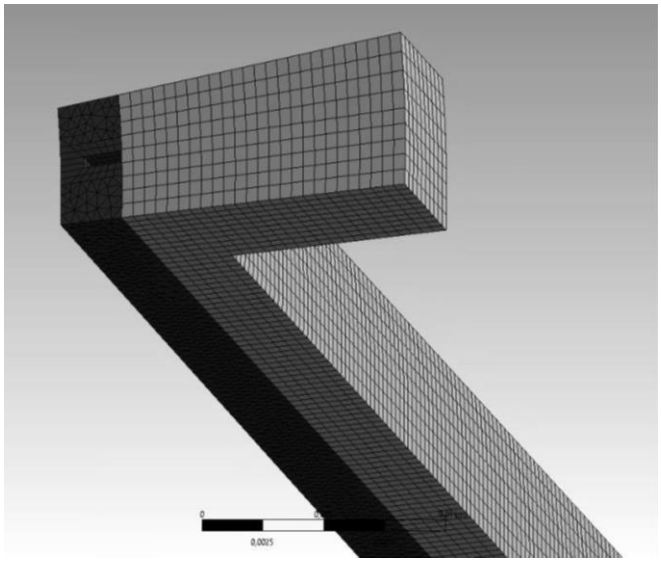

Figure 6: Mesh around a single channel

DOI: 10.13009/EUCASS2022-7676

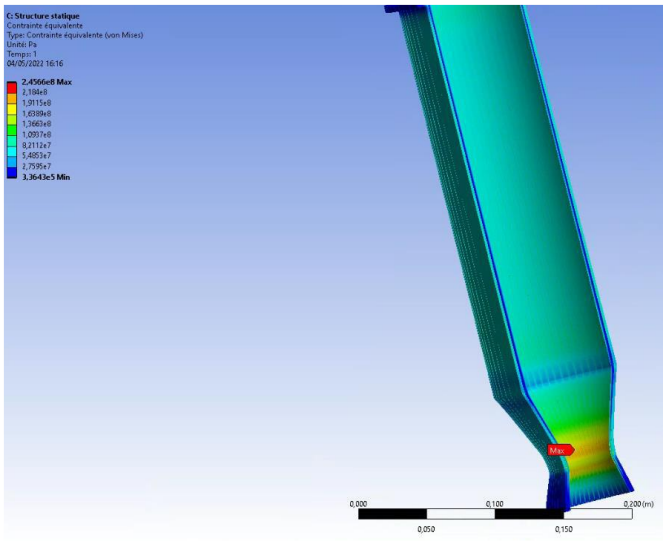

Figure 7: Mechanical constraints along the engine

4.5. Pressure drop inside the regenerative cooling circuit

As this engine does not have any turbopumps, the fuel and oxidizer are pressurized inside the tanks. This means that pressure loss in the circuit should be minimized since a higher pressure implies the use of heavier tanks. Therefore, it is crucial to ensure that the pressure at the end of the regenerative cooling circuit is sufficient for the injection system to work properly. The flow between the main pipe coming from the methane tank and the end of the cooling channels is simulated using ANSYS Fluent to determine the pressure drop between these two points. The flow is first divided into 2 equal half-tori that each distributes the flow into 10 identical conduits that are then each divided in three equal cooling channels that then run from below the chamber throat up to the injection plate. The pressure loss for the current design is 16.8 bars, which will have to be lowered in later revisions.

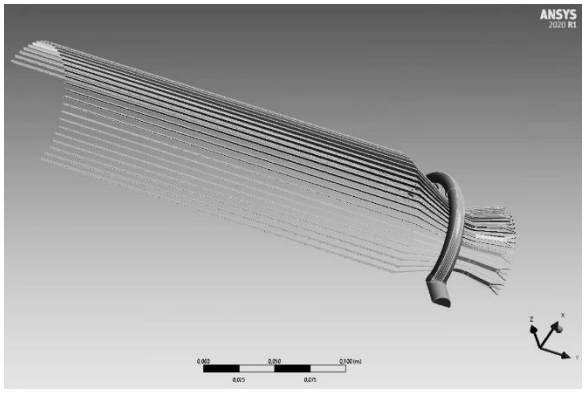

Figure 8: Geometry of half the regenerative cooling circuit

DOI: 10.13009/EUCASS2022-7676

5. Adaptative nozzle

The adaptive exit cone meets the need to adapt a rocket engine to its operating altitude. The objective is to demonstrate the effectiveness of this innovation through the creation of the Mini Viserion. The principle is simple: to vary the cross-sectional area of the rocket engine nozzle in a continuous manner. The thrust (8) and gas ejection velocity (9) equations show that the only way to maximise thrust for a given propellant flow rate is to cancel the pressure dependent term in (8). According to equation (10), the ratio of ejection pressure to combustion chamber pressure varies with the output Mach number. To influence the ejection pressure, it is necessary to vary the number of Mach at the outlet, which is defined by equation (11) as a function of ε, the ratio of the outlet cross-sectional area to the nozzle throat area.

$$F = iV_e + S_e(P_e - P_{amb}) \tag{8}$$

$$V_e = \sqrt{\frac{2\gamma}{\gamma - 1}\frac{8314}{m}T_c\left(1 - \left(\frac{P_e}{P_c}\right)^{\frac{\gamma-1}{\gamma}}\right)} \tag{9}$$

$$\frac{P_e}{P_c} = \left(1 + \frac{\gamma - 1}{2}M^2\right)^{\frac{-\gamma}{\gamma-1}} \tag{10}$$

$$\varepsilon = \frac{S_e}{S_c} = \frac{1}{M_e}\left[\frac{\left(1 + \frac{\gamma - 1}{2}\right)M_e^2}{\frac{(\gamma + 1)}{2}}\right]^{\frac{\gamma+1}{2(\gamma-1)}} \tag{11}$$

Within the context of the Mini Viserion project, it is necessary to start with an outlet pressure equal to the pressure at sea level and then reduce it by lengthening the nozzle gradually in order to increase its expansion ratio, therefore keeping the nozzle adapted (i.e., keeping the output pressure close to the ambient pressure) for as long as possible.

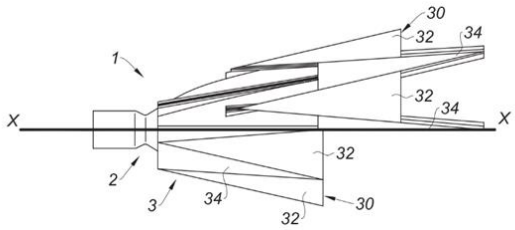

Figure 9: Half-view of the mechanism extended and retracted

The half-view in Figure 9 shows the mechanism in both the extended (top) and retracted (bottom) positions. It is an assembly of curved triangular tiles, connected to each other by linear rails, forming a frustoconical ring when assembled. Each tile is also connected to the nozzle body by a rail allowing its guidance. The deployment device is not visible on this figure but can be envisaged in several ways depending on the thrust range of the engine. In the case of the Mini Viserion, the pressure in the chamber is not very high and the "fixed" divergent section remains quite short. The geometric dimensioning of the adaptive nozzle can only be done at about 75% of its optimal capacity. The associated variable outlet pressure range is therefore 1 to 0.55 bar. The lack of space on a fixed diverter of this size also makes it difficult to use regenerative circuit channels to cool its end.

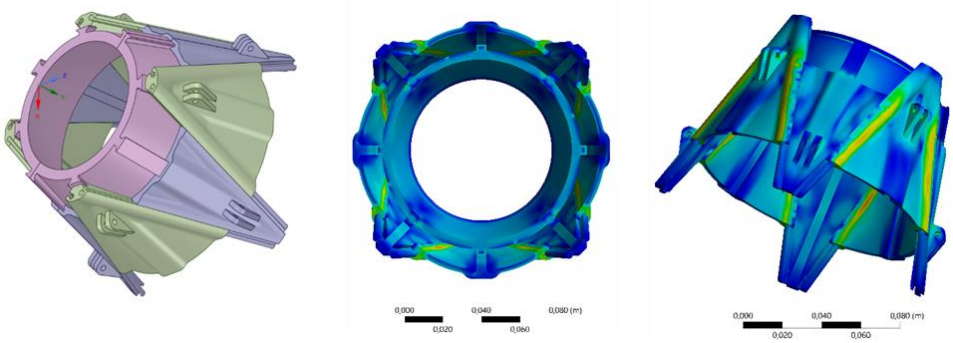

Figure 10: Adaptive nozzle assembly and numerical simulation of stresses

DOI: 10.13009/EUCASS2022-7676

The proposed assembly is therefore the one shown in Figure 10, i.e., an assembly of 8 tiles on a fixed nozzle. Given the temperatures and convection coefficients to which the system is exposed, silicon carbide (SiC) was chosen as the material for the tiles and the fixed divergent. This material is also preferred because of its low thermal expansion and its mechanical strength even at high temperatures. These parts are not actively cooled, and the heat flow is only removed by radiation, that is by radiative cooling. The equation used (12) predicts the maximum temperature reached, which is obviously at the gas side wall. Based on the emissivity of SiC, which varies between 0.86 and 0.94, the results show a peak temperature of around 2100 K. SiC is known to have a particularly high heat resistance (over 1900°C), however, it is subject to ablation. The effects of ablation depend on the duration during which the SiC is exposed to these high temperatures. As the use of a rocket engine is rarely more than a few minutes of operation, this material is impeccably suited to our design.

$$q = \varepsilon \sigma {T_{wg}}^4 \tag{12}$$

In order to allow the tiles to move, it is necessary that the surface roughness of the different rails be sufficiently low. Fortunately, the set of vibrations generated during the firing process plays a significant role in the deployment. The latter is ensured by 4 electric actuators, each of which activates a ring in pairs. In figure 11, the rings (in red and purple) are connected to the tiles by means of rods. By moving the two rings proportionally, the actuators allow the tiles to be deployed precisely and simultaneously.

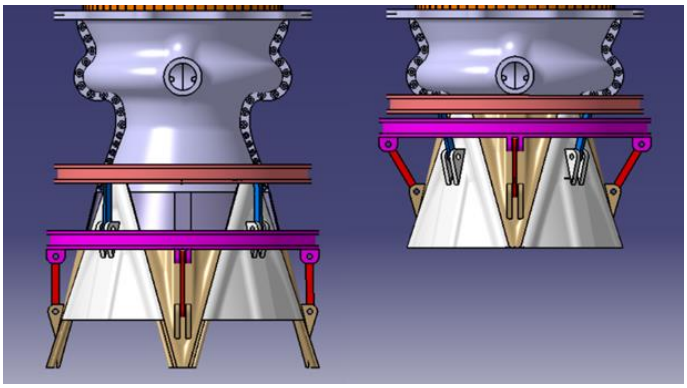

Figure 11: Deployment mechanism assembly

6. Thrust Vector Control

The Mini Viserion is a rocket engine designed to equip the Astreos rockets of the PERSEUS project. In practice, it is necessary for this motor to be able to change orientation in order to modify the direction of the thrust vector and thus be able to direct the rocket. To enable TVC, the engine needs to be mounted on a base which not only allows rotation on two axes, but that is equipped with an actuation device capable of performing those rotations. Seeing that the motor is already equipped with 4 electric cylinders, the objective is to make use of these same cylinders to orientate the engine. This means that no additional weight is added. We will first detail the design of the gimbal, then the thrust plate on which the gimbal and the cylinders are fixed.

6.1. Design of the gimbal

According to the state of the art, two main types of bases correspond to our needs. The first is the use of a gimbal while the second is the use of a ball-and-socket joint. In both cases, the mobility of the engine is not affected. However, it was soon determined that the gimbal best suited our needs. Indeed, the inlet for one of the propellants (LOX) is located at the top of the engine and the use of a ball joint would prevent the passage of the flexible hose that supplies the pintle. A gimbal, on the other hand, is more adaptable and allows a hole to be left in its center for the LOX pipe. Consequently, several designs were considered and optimized. The first version in Figure 12 (middle) is directly derived from the gimbal presented by Huzel and Huang (left) [6].

DOI: 10.13009/EUCASS2022-7676

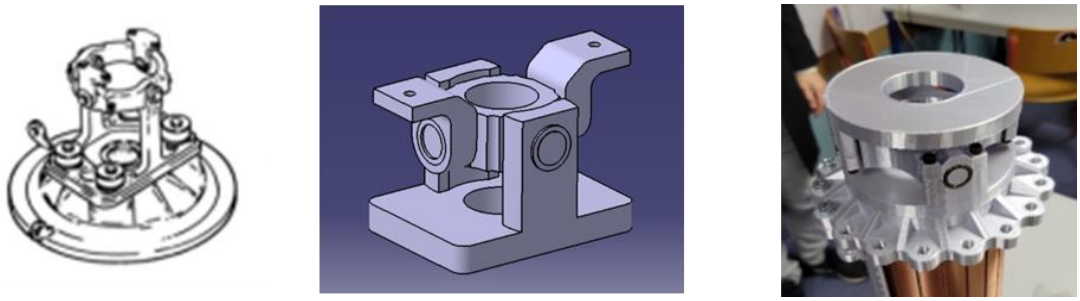

Figure 12: Evolution and optimisation of the gimbal design

The next version can be seen 3D printed in Figure 12 (right). It shows some improvements for a better interface with the motor, such as a circular base. In addition, the assembly has been thought out to allow the placement of the roller bearings. These bearings can withstand 6 kN of radial thrust each, which is plentiful. A final set of optimizations were adopted later and are visible in Figure 13. The whole assembly has been considerably lightened and redesigned for simpler machining. The central hole was also enlarged to ensure the necessary space for the flexible LOX pipe. The base of the struts has also been widened to increase the mechanical strength, especially when the inclination of the engine varies. Finally, the height of the struts has been adjusted to achieve the desired 10° of travel.

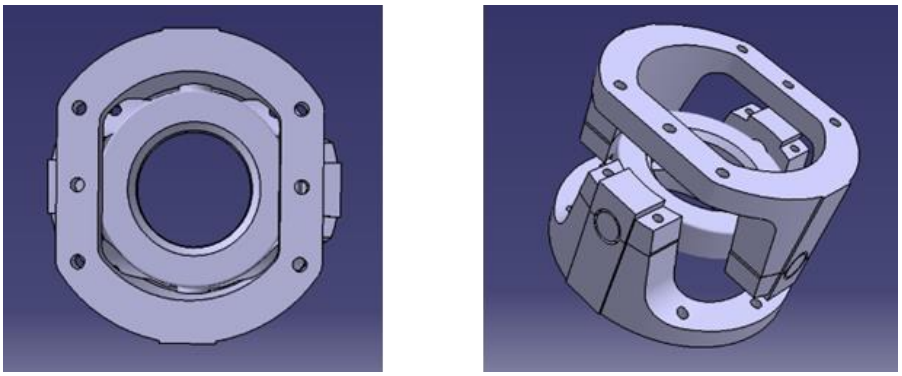

Figure 13: Views of the final gimbal assembly

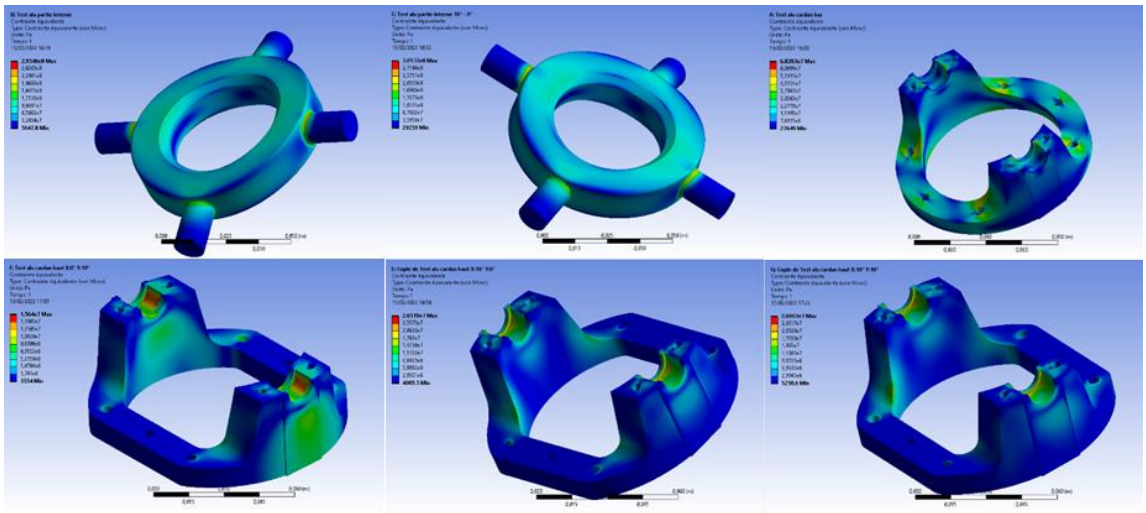

Figure 14: Graph of results of numerical mechanical simulations of Von mises equivalent stresses

In order to preserve the total mass of the engine, the lightest viable material was chosen, aluminum 7075 T6, which has a yield strength of 500 MPa. Numerical mechanical studies at various thrust angles were realized and the results are shown in Figure 14. The results are shown at the top left for an angle of 0°, then in the middle at the top for an angle of 10°. The top right picture corresponds to the case where the lower part of the gimbal is aligned with the motor, so the thrust stays axial. The bottom images correspond to the upper part of the gimbal, with on the left a 10° tilt along the Y axis of the bearings, in the middle 10° tilt along the X axis, then on the right the gimbal is

DOI: 10.13009/EUCASS2022-7676

rotated by 10° in both the X and Y directions. The measured stresses are the equivalent Von Mises stresses which are equal to 305MPa at most therefore these results are satisfying, with a safety factor of 1.64.

6.2. Design of the thrust plate

As the engine will eventually be fixed to the 250mm internal diameter rocket body, an adaptor is still needed to interface with the gimbal. Moreover, it is also on this part that the base of the 4 electric cylinders must be fixed. The design ultimately resulted in the creation of two plates in order to divide the attachment between two points and ensure greater rigidity. The proposed design still uses the same alloy as the gimbal and was designed to facilitate machining while maintaining a certain lightness. Figure 15 shows the planned assembly with a ball-and-socket joint to allow for cylinder deflection. Figure 16 shows the result of the numerical mechanical simulation of the overall assembly.

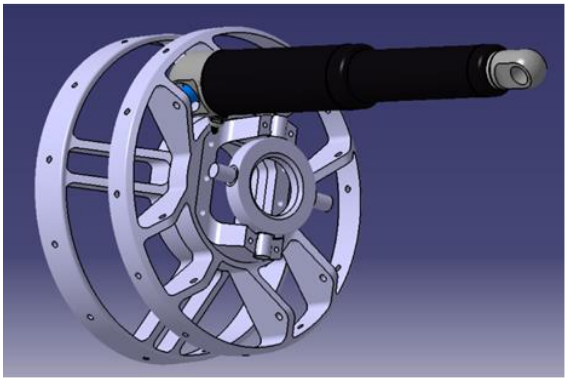

Figure 15: Assembly with ball bearing actuator

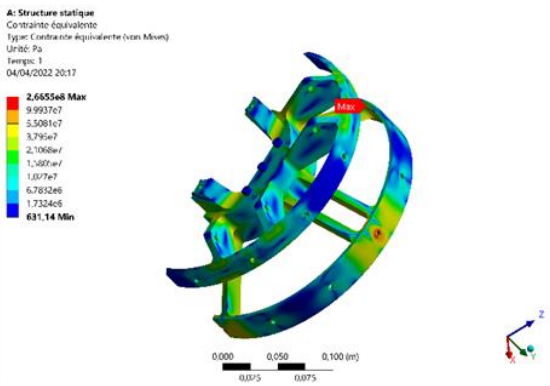

Figure 16: Graph of stress results on the assembly

7. Conclusion and perspective

This paper has presented the current progress made on the Mini Viserion's injection system, cooling system and adaptative nozzle. The creation of a water test bench for testing the injection system is planned in the near future. Thanks to that, atomization and mass flow tests will be conducted. Concerning the regenerative cooling system, the search for materials suppliers has started. Finally, the development of an ignition system for the engine has already begun and will be the focus of the upcoming months. Given the importance of nozzle adaptability in increasing the efficiency of future rocket engines, the Innovative Propulsion Laboratory is proud of the progress made by its volunteers in the last two years with respect to that subject. Once tested and its efficiency demonstrated on the Mini Viserion engine, this innovative nozzle design has potential for wide applicability in upcoming rocket engines. The interest of the CNES for our extensible nozzle design as well as the integration of the IPL in the PERSEUS project are tokens of the trust and support professionals have regarding our projects.

Acknowledgements

We would like to thank the CNES and the PERSEUS project for the trust they put in our team, as well as for their precious financial and technical support in addition to their valuable guidance in this project. We also thank IPSA, our university, for their logistical and financial support. Thanks to the support of all these partners, the Innovative Propulsion Laboratory keeps growing and improving its skills.

References

[1] CNES. 2020. Spécification moteur Mini Viserion.
[2] P. Pempie. CNES. Moteur Fusée à ergols liquides. VII: 152-158.
[3] E. Mercieca. 2017. Spray Characteristics in Gas / Liquid Pintle Injection
[4] A. Trujillo. 2014. An Experimental Investigation on Liquid Methane Convection and Boiling in Rocket Engine Cooling Channels. University of Texas at El Paso.
[5] J. Van Noord. 2010. A Heat Transfer Investigation of Liquid and Two-Phase Methane. Glenn Research Center.
[6] D.K Huzel, D.H. Huang. 1967. Design of Liquid Propellant Rocket Engines, Second Edition